ChemComm

COMMUNICATION

View Article Online
View Journal | View Issue



Cite this: *Chem. Commun.*, 2018, **54**, 8056

Received 21st May 2018,
Accepted 24th June 2018

DOI: 10.1039/c8cc04058c

rsc.li/chemcomm



# Reactive two-component monolayers template bottom-up assembly of nanoparticle arrays on HOPG†

Chen Fang, Hua Zhu, Ou Chen and Matthew B. Zimmt *

**Two triphenyleneethynylene derivatives, $1^{OH}$ and 2, self-assemble a patterned monolayer (ML) at the solution–graphite (HOPG) interface. The four molecule unit cell of the ML, ($1^{OH}1^{OH}$22), spans 19 nm and contains adjacent columns of $1^{OH}$ molecules spaced by 4.7 nm. Following ML assembly, a disulfide is appended to the alcohol group on each $1^{OH}$ molecule and used to capture 2.0 nm gold nanoparticles (AuNP). The patterned monolayer directs bottom-up assembly of a 5 nm/19 nm double pitch AuNP pattern.**

Designed monolayers (ML) expressing compositional patterns assemble spontaneously on planar surfaces from multi-component solutions.[1–5] Incorporating distinct reactivity in the components of pattered monolayers should allow these assemblies to function as ultra-high resolution templates.[6,7] Surfaces with controlled nanometer spacing of nano-objects could find use in electronic, optical, magnetic or analytical applications. Assembly of surfaces with designed patterns of different size nanoparticles has been demonstrated on mica[8] using DNA Origami.[9] Nanoparticle capture on polymer[10] or physisorbed monolayer surfaces affords various levels of organization, from random[11] to well aligned assemblies.[12–14] A related strategy underlies directed self-assembly lithography, which yields features with sub-10 nm pitch.[15–17] Here we employ time of flight mass spectrometry (TOF-MS) and scanning probe microscopies (STM, AFM) to demonstrate the self-assembly, chemical functionalization and application of a two-component patterned monolayer as a template to direct gold nanoparticle (AuNP) surface assembly into columns with 5 nm and 19 nm spacing patterns. Extending this strategy to other of multi-component ML systems[1–7] will enable bottom-up fabrication of increasingly complex nano-object assemblies.

*Department of Chemistry, Brown University, Providence, RI 02912, USA. E-mail: mbz@brown.edud*

† Electronic supplementary information (ESI) available: General protocols, synthesis of AuNP, $1^{OH}$ and 2, statistical summaries of MS intensities from independent samples, TOF-MS from each spot sampled on each drop cast ML and on each ML formed following surface reactions, STM and AFM images of ($1^{OH}1^{OH}$22) monolayer after DBTP modification and AuNP incubation. See DOI: 10.1039/c8cc04058c

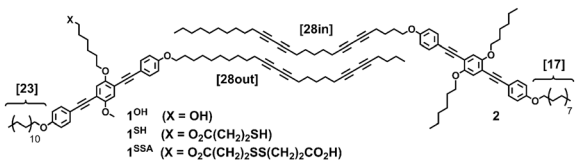


Fig. 1 TPE compounds used to self-assemble patterned monolayers (ML) with a four molecule unit cell, ($1^{OH}1^{OH}$22). Reactions at the ML – solution interface convert $1^{OH}$ into $1^{SSA}$, $1^{SH}$ and $1^{SS}1$ (not shown).

Two triphenyleneethynylene (TPE) molecules, $1^{OH}$ and 2 (Fig. 1), were designed to assemble monolayers comprised of two adjacent columns of $1^{OH}$ molecules alternating with two adjacent columns of 2 molecules (($1^{OH}1^{OH}$22) unit cell). $1^{OH}$ and 2 contain long side chains with different shapes and lengths to direct self-assembly of the patterned ML morphology. Molecule $1^{OH}$ has one "linear" docosyloxy side chain, [23], and one "bumped" heptacosa-11,13,20,22-tetrayn-1-yloxy side chain, [28out], attached at opposing terminal *para*-positions of a TPE unit. The central benzene ring of $1^{OH}$ has two "core chains"; a methoxy group *ortho* to the aryl ring bearing the [23] side chain and a 6-hydroxyhex-1-yloxy chain *ortho* to the aryl ring bearing the [28out] side chain. The terminal hydroxyl group on the $1^{OH}$ core chain is the site of ML reaction and template function. Molecule 2 has a "linear" hexadecyloxy side chain, [17], and a "bumped" heptacosa-5,7,14,16-tetrayn-1-yloxy side chain [28in] at opposing *para*-positions of the TPE. The central benzene ring of 2 has two, *para* hexyloxy core chains.

The TPE molecules' two long side chains extend in opposite directions. These side chains assemble aliphatic lamellae by interdigitating with shape- and length-complementary side chains from an adjacent column of TPE units. Close packing of complementary side chains within aliphatic lamellae stabilizes assembly of the intended ML morphology. Segregation of [17] and [23] chains into separate lamellae maximizes van der Waals interactions for both side chains. Interdigitation of [17] side chains drives assembly of two adjacent columns of 2 molecules. Likewise, interdigitation of [23] side chains directs assembly of

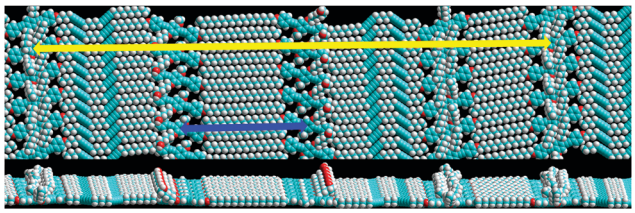

Fig. 2 Top: Molecular mechanics minimized section of ($\mathbf{1}^{OH}\mathbf{1}^{OH}$**22**) morphology ML on HOPG. The unit cell repeat spans 18.8 nm (yellow arrow). The center-to-center distance between nearest $\mathbf{1}^{OH}$ columns is 4.7 nm (blue arrow). Bottom: ML section side view.

analogous "double columns" of $\mathbf{1}^{OH}$ molecules. The off-center locations of the "tetrayne-bumps" in [28in] and [28out] make this side chain pair shape-complementary but make each side chain shape self-incommensurate. Aliphatic lamellae containing tetrayne-bump chains maximize van der Waals stabilization by packing each [28] chain between two copies of the other [28] chain. This directs assembly of $\mathbf{1}^{OH}$ and **2** columns on opposite edges of each tetrayne chain lamella. Molecular mechanics modeling predicts the ($\mathbf{1}^{OH}\mathbf{1}^{OH}$**22**) morphology separates the centers of TPE units in adjacent $\mathbf{1}^{OH}$ columns by 4.7 nm. The unit cell repeat (Fig. 2) enforces a separation of 18.8 nm between the centers of neighboring $\mathbf{1}^{OH}$ "double columns".

Monolayers of $\mathbf{1}^{OH}$ and **2** were assembled on highly oriented pyrolytic graphite (HOPG) from equimolar solutions (5–20 μM in phenyloctane (PO)). Scanning tunneling microscopy (STM) images collected from the solution–HOPG interface revealed assembly of two different ML morphologies (Fig. 3a). The dominant morphology exhibited the desired ($\mathbf{1}^{OH}\mathbf{1}^{OH}$**22**) pattern, with a ML repeat containing four aliphatic lamellae. The second morphology, observed infrequently and with poor resolution, exhibited only two aliphatic lamellae per repeat, one of which was narrower than any aliphatic column in the ($\mathbf{1}^{OH}\mathbf{1}^{OH}$**22**) morphology. The incidence of this minor morphology varied from sample to sample. Surprisingly, solutions of $\mathbf{1}^{OH}$ applied to HOPG exhibited MLs in STM scans, despite the absence of the shape complementary bumped-tetrayne

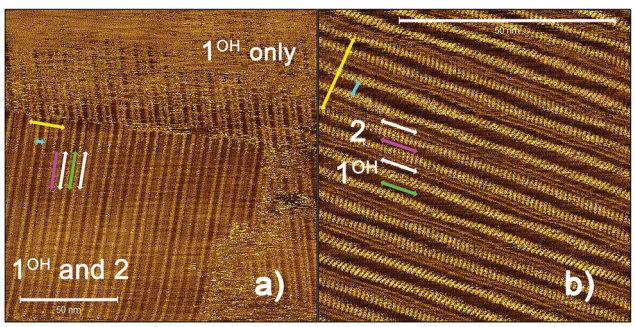


Fig. 3 STM images of drop cast $\mathbf{1}^{OH}$/**2** ML on HOPG. Arrows mark features of the ($\mathbf{1}^{OH}\mathbf{1}^{OH}$**22**) patterned domains: the 19 nm repeat (yellow), the center-to-center distance between nearest $\mathbf{1}^{OH}$ columns (cyan), [17] lamella (magenta), bumped tetrayne lamella (white), [23] lamella (green). Scale bars 50 nm. (a) ML drop cast from 10 μM $\mathbf{1}^{OH}$/10 μM **2** solution (160 nm × 160 nm) contains both patterned (lower left) and $\mathbf{1}^{OH}$-only domains. (b) ML drop cast from 4 μM $\mathbf{1}^{OH}$ and 6 μM **2** solution (72 nm × 72 nm) contains only the ($\mathbf{1}^{OH}\mathbf{1}^{OH}$**22**) patterned morphology.

side chain from **2**. $\mathbf{1}^{OH}$ MLs exhibited the same lamellar pattern (Fig. S1, ESI†) as the minor morphology formed from equimolar $\mathbf{1}^{OH}$/**2** solutions. The two long side chains on $\mathbf{1}^{OH}$ ([23] and [28out]) afford this molecule a physisorption advantage, enabling it to assemble single component ML domains in competition with the two component, patterned domains. Adjusting $\mathbf{1}^{OH}$ and **2** concentrations and ratios might counteract this advantage so that only the ($\mathbf{1}^{OH}\mathbf{1}^{OH}$**22**) morphology assembles (*vide infra*).

STM must be used to verify morphologies assembled by multi-component ML, but this technique samples small areas (<1 μm$^2$) and is slow. Time-of-flight mass spectrometry (TOF-MS) rapidly analyses much larger areas of MLs assembled on HOPG[18] (>2000 μm$^2$ per irradiated spot), providing relative compositions of multi-component ML convolved with a response factor for each component.[19] Preparation conditions that assemble only the patterned ($\mathbf{1}^{OH}\mathbf{1}^{OH}$**22**) morphology ML should produce the same, constant value of the $\mathbf{1}^{OH}$:**2** TOF-MS intensity ratio. TOF-MS can rapidly screen ML composition as a function of different $\mathbf{1}^{OH}$ and **2** solution concentrations to identify promising mixtures. STM can then be used to ascertain the specific ML morphology assembled by these mixtures. Accordingly, $\mathbf{1}^{OH}$:**2** TOF-MS intensity ratios were determined at multiple locations of HOPG substrates prepared from various $\mathbf{1}^{OH}$ and **2** solution concentrations and ratios.

Samples for TOF-MS analyses were prepared by applying 6 μL of $\mathbf{1}^{OH}$/**2** solution on freshly cleaved HOPG (12 mm × 12 mm) at 19 °C. After sitting 15 minutes, the HOPG substrate was rinsed with was rinsed with 25 μL PO and then hexane (3 × 25 μL). A thin film of the MALDI matrix 2,4,6-trihydroxyacetophenone (THAP) was applied (15 μL 1.7 mg mL$^{-1}$ THAP in 30% acetone/octane) to the HOPG substrate to increase TOF-MS signal intensities. TOF-MS determined $\mathbf{1}^{OH}$:**2** ion[20] intensity ratios (Table 1, Fig. 4 and Fig. S2, ESI†) exhibited a plateau value of 0.42 for applied PO solutions containing 3 or 4 μM $\mathbf{1}^{OH}$ and 50–100% higher **2** concentrations (4.5–8 μM).[21] Larger, more variable $\mathbf{1}^{OH}$:**2** TOF-MS intensity ratios arose using higher concentrations of $\mathbf{1}^{OH}$ (*e.g.* 10 μM) or higher relative concentrations of $\mathbf{1}^{OH}$ (equimolar or higher). These latter solutions assembled ML on HOPG with "excess" $\mathbf{1}^{OH}$. This concurs with STM observation of single component $\mathbf{1}^{OH}$ domains in addition to patterned ($\mathbf{1}^{OH}\mathbf{1}^{OH}$**22**) domains from equimolar $\mathbf{1}^{OH}$/**2** solutions. STM images of ML prepared by drop casting 4 μM $\mathbf{1}^{OH}$/6 μM **2** solutions exhibited patterned ($\mathbf{1}^{OH}\mathbf{1}^{OH}$**22**) domains (Fig. 3b) but no evidence of single component $\mathbf{1}^{OH}$ domains.[21] This solution composition was used to prepare ML for AuNP template studies.

Patterned ($\mathbf{1}^{OH}\mathbf{1}^{OH}$**22**) ML on HOPG was esterified[22] with 3,3′-dithiobispropanoic acid (DTBP) to append a disulfide group on the $O(CH_2)_6OH$ core chain of $\mathbf{1}^{OH}$ and to promote AuNP capture ($O(CH_2)_6O_2C(CH_2)_2$S-S-R, see Reaction Protocol 1, ESI†). DTBP esterification can (i) cross-link $\mathbf{1}^{OH}$ molecules within the

Table 1 $\mathbf{1}^{OH}$:**2** surface TOF-MS intensity ratio *versus* solution composition

| [$\mathbf{1}^{OH}$]:[**2**] sol'n ratio | 2:1 | 1:1 | 1:1.5 | 1:2 |
|---|---|---|---|---|
| [$\mathbf{1}^{OH}$] = 4 μM | 1.01 ± 0.37 | 0.51 ± 0.11 | 0.42 ± 0.06 | 0.40 ± 0.07 |
| [$\mathbf{1}^{OH}$] = 3 μM | 0.81 ± 0.24 | 0.45 ± 0.08 | 0.43 ± 0.07 | 0.41 ± 0.06 |

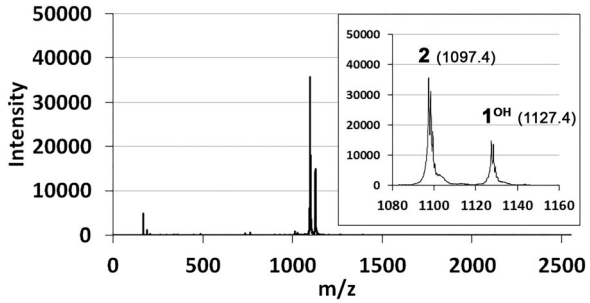


Fig. 4 TOF-MS of ML assembled on HOPG from 6 μL phenyloctane containing 6 μM **2** and 4 μM $\mathbf{1}^{OH}$. A thin THAP film ($m/z$ = 169 $[M + H]^+$) was applied to the ML to increase signal intensities. Inset: Expansion of the **2** and $\mathbf{1}^{OH}$ peak region. This sample's $\mathbf{1}^{OH}$ : **2** intensity ratio is 0.42.[21] See Fig. S2 (ESI†) for all TOF-MS data from drop cast solutions.

same TPE column, forming dimeric $TPE_2$ linked by a disulfide, $\mathbf{1}^{SS}\mathbf{1}$, or (ii) form a core chain containing a disulfide group and a terminal carboxylic acid, $\mathbf{1}^{SSA}$ (Fig. 1). TOF-MS spectra collected after rinsing the ML and applying a thin THAP film (Fig. 5a, b and Fig. S3, ESI†) exhibited normal intensity from **2** (ion intensity $\sim 3 \times 10^4$) but less than 5% of the previous $\mathbf{1}^{OH}$ intensity ($\mathbf{1}^{OH}$ : **2** int. ratio = 0.02 ± 0.01). TOF-MS measurements at higher laser power (LP), required to detect heavier and less intense species,[23] revealed (Fig. 5c, d and Fig. S4, ESI†) a low intensity peak at $m/z \sim 2432$ assigned as $TPE_2$ $\mathbf{1}^{SS}\mathbf{1}$ (ion intensity <600) and a low intensity peak at $m/z$ = 1320 assigned as $\mathbf{1}^{SSA}$ (ion intensity <1000).[20] $TPE_2$ dimers adhere more strongly to HOPG than TPE monomers.[19] Comparable TOF-MS intensities from $\mathbf{1}^{SS}\mathbf{1}$ and $\mathbf{1}^{SSA}$ indicates ML cross-linking competes favourably with "bimolecular" reaction between solution DTBP and $\mathbf{1}^{OH}$ in the ML.[24] DTBP reacted ML were not imageable by STM.[25]

The dimeric nature of the $\mathbf{1}^{SS}\mathbf{1}$ peak was confirmed by reduction of the disulfide cross-link with dithiothreitol (DTT).[26] After treating DTBP-reacted ($\mathbf{1}^{OH}\mathbf{1}^{OH}$**22**) ML with DTT (see Reaction Protocol 2, ESI†), the peaks attributed as $\mathbf{1}^{SS}\mathbf{1}$ and $\mathbf{1}^{SSA}$ were absent from TOF-MS spectra (Fig. S5, ESI†). A new peak observed at $m/z$ = 1216. (Fig. 5e and Fig. S5, ESI†) was assigned as $\mathbf{1}^{SH}$, a TPE bearing a thiol-terminated core chain ($O(CH_2)_6O_2C(CH_2)_2SH$, Fig. 1).[20] The $\mathbf{1}^{SH}$ peak intensity was roughly 10% as large as the non-reactive ML molecule **2** ($\mathbf{1}^{SH}$ : **2** int. ratio = 0.11 ± 0.01). This intensity ratio was much smaller than the starting $\mathbf{1}^{OH}$ : **2** ratio (0.42), which could indicate loss of $\mathbf{1}^{OH}$ derived compounds due to cross-linking. To estimate relative TOF-MS response factors for $\mathbf{1}^{SH}$ and **2**, the former was prepared from patterned ($\mathbf{1}^{OH}\mathbf{1}^{OH}$**22**) ML by a route that avoided cross-linking. The ($\mathbf{1}^{OH}\mathbf{1}^{OH}$**22**) ML was esterified using the mono-ethyl ester of 3,3′-dithiobispropanoic[27] and reduced with DTT (see Reaction Protocols 3 and 4, ESI†). The $\mathbf{1}^{SH}$ : **2** int. ratio generated by this surface reaction, 0.09 ± 0.01 (Fig. S6, ESI†), was similar to the ratio following reduction of DTBP cross-linked ML. This indicates reasonable retention of $\mathbf{1}^{OH}$ compounds during cross-linking and a four-fold smaller response factor for $\mathbf{1}^{SH}$ than for $\mathbf{1}^{OH}$.[28]

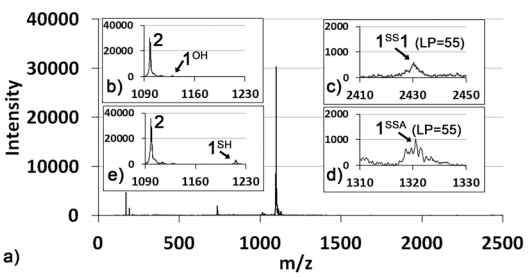


Fig. 5 TOF-MS after surface reactions and application of a thin THAP film. (a) Spectrum (0–2.5 kD, laser power (LP) = 47%) after esterification of $\mathbf{1}^{OH}$ with DTBP. (b) Expansion of (a) showing reduced intensity of $\mathbf{1}^{OH}$ after DTBP surface reaction. (c) TOF-MS (LP = 55%) of dimer region after DTBP surface reaction. (d) TOF-MS (LP = 55%) of $\mathbf{1}^{SSA}$ region after DTBP surface reaction. (e) TOF-MS (LP = 47%) of monomer region after DTT reduction of DTBP esterified ML.

For AuNP capture studies, ($\mathbf{1}^{OH}\mathbf{1}^{OH}$**22**) ML was esterified with DTBP to install disulfide groups on $\mathbf{1}^{OH}$ columns and then incubated with 2 nm diameter AuNP stabilized with oleylamine surface coatings;[29] the weak amine–gold bond should facilitate capture of AuNP by ML disulfide groups. Patterned ML were incubated for 15–60 minutes in hexane (1 mL) containing 5 μg of AuNP and then rinsed, dropwise, with 2 mL of hexane. STM images displayed AuNP patterns consistent with the designed ML template. High resolution STM scans (Fig. 6b) resolved double AuNP columns, with ~5 nm spacing of proximate AuNP columns. The 1-D height autocorrelation function (ACF)[30] (Fig. 6a) calculated perpendicular to the AuNP columns in the STM image exhibit maxima at intervals of ~19 nm. Less distinct shoulders are present at distances ~5 nm shorter and longer than the 18.8 and 37.6 nm maxima. Both features are consistent with the double column morphology of the underlying ($\mathbf{1}^{OH}\mathbf{1}^{OH}$**22**) ML. Additional STM images (Fig. S7, ESI†) confirmed assembly of AuNP columns with the 5 nm/19 nm double column morphology.

Large area tapping mode AFM images collected at the air–HOPG interface (Fig. 6c) revealed roughly linear strips spaced by 20 ± 1 nm, with 10 ± 2 nm FWHM and 1.5–2 nm height modulation. The strips are assigned as doubled AuNP columns templated by the ML as no comparable features were observed

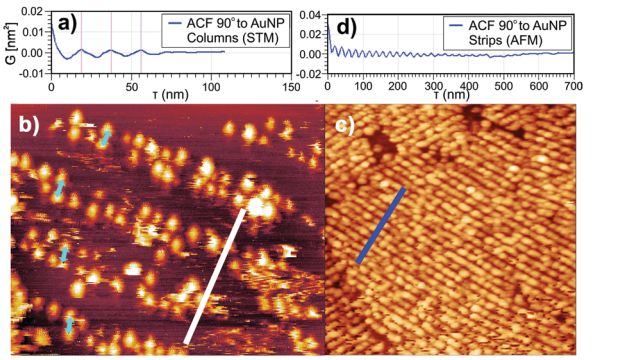


Fig. 6 (a) 1-D height autocorrelation function (ACF)[30] of STM image perpendicular to AuNP columns (white bar in b). Pink lines mark maxima at 18.8, 37.6 and 56.1 nm. (b) STM image (100 nm × 75 nm) of DTBP reacted ($\mathbf{1}^{OH}\mathbf{1}^{OH}$**22**) ML after incubation with 2 nm AuNP. Cyan arrows mark 5 nm. (c) 0.6 μM × 0.6 μM AFM image of DTBP modified ($\mathbf{1}^{OH}\mathbf{1}^{OH}$**22**) ML after incubation with 2 nm AuNP. The bright strips are captured AuNP. (d) 1-D height autocorrelation function (ACF)[30] of AFM image perpendicular (blue bar in c) to the AuNP strips. Maxima are spaced by 20 ± 1 nm.

in AFM images collected from ($\mathbf{1}^{OH}\mathbf{1}^{OH}$**22**) MLs on HOPG or from ($\mathbf{1}^{OH}\mathbf{1}^{OH}$**22**) MLs exposed to AuNP without DTBP modification.[31] The radius of the AC240TS-R3 AFM probe (7 nm) did not afford sufficient resolution to verify that each strip is composed of double AuNP columns spaced by 5 nm. AFM visualized domains contained 10–30 parallel strips and approached 500 nm in length. The 1-D height autocorrelation function (ACF)[30] orthogonal to the AuNP strip direction exhibited more than fifteen maxima spaced by 19–20 nm. Strip orientations in adjacent domains differed by $\sim 60^{\circ}$, indicating that the underlying HOPG symmetry axes control alignment of AuNP assemblies by directing ($\mathbf{1}^{OH}\mathbf{1}^{OH}$**22**) ML domain orientations.[32] The AFM studies confirm ML mediated, bottom-up assembly of AuNP structures with a 19 nm repeat.

In conclusion, STM and TOF-MS were used to identify preparation conditions that optimize self-assembly of ($\mathbf{1}^{OH}\mathbf{1}^{OH}$**22**) patterned MLs. Patterned ML assembly was driven by length and shape dependent interactions of TPE side chains. TOF-MS was used to verify the subsequent covalent modification of $\mathbf{1}^{OH}$ molecules with a disulfide group at the ML – solution interface. STM and AFM imaging demonstrated that disulfide modified MLs effectively translate patterned ML morphology into a bottom-up template, directing surface assembly of AuNP into 5 nm spaced doubled columns with an overall 19 nm repeat.

This work was supported by the U.S. National Science Foundation grant number CHE1607273. Assistance with mass spectrometry from Dr Tun-Li Shen, Ken Talbot and Randy Goulet, with NMR from Dr Hopson and with AFM from Dr Hector Garces is acknowledged gratefully.

## Conflicts of interest

There are no conflicts to declare.

## Notes and references

1 J. A. Theobald, N. S. Oxtoby, M. A. Phillips, N. R. Champness and P. H. Beton, *Nature*, 2003, **424**, 1029–1031.
2 G. Velpula, T. Takeda, J. Adisoejoso, K. Inukai, K. Tahara, K. S. Mali, Y. Tobe and S. De Feyter, *Chem. Commun.*, 2017, **53**, 1108–1111.
3 Z.-F. Cai, T. Chen, J.-Y. Gu, D. Wang and L.-J. Wan, *Chem. Commun.*, 2017, **53**, 9129–9132.
4 Y. Xue and M. B. Zimmt, *J. Am. Chem. Soc.*, 2012, **134**, 4513–4516.
5 A. Ciesielski, C.-A. Palma, M. Bonini and P. Samori, *Adv. Mater.*, 2010, **22**, 3506–3520.
6 Y. L. Huang, W. Chen and A. T. S. Wee, *J. Am. Chem. Soc.*, 2011, **133**, 820–825.
7 K. Tahara, K. Nakatani, K. Iritani, S. De Feyter and Y. Tobe, *ACS Nano*, 2016, **10**, 2113–2120.
8 Y. Y. Pinto, J. D. Le, N. C. Seeman, K. Musier-Forsyth, T. A. Taton and R. A. Kiehl, *Nano Lett.*, 2005, **5**, 2399–2402.
9 P. W. K. Rothemund, *Nature*, 2006, **440**, 297–302.
10 R. Shenhar, T. B. Norsten and V. M. Rotello, *Adv. Mater.*, 2005, **17**, 657–669.
11 X. Wei, W. Tong, V. Fidler and M. B. Zimmt, *J. Colloid Interface Sci.*, 2012, 221–227.
12 M. A. Mezour, I. I. Perepichka, J. Zhu, R. B. Lennox and D. F. Perepichka, *ACS Nano*, 2014, **8**, 2214–2222.
13 S.-B. Lei, C. Wang, S.-X. Yin, L.-J. Wan and C.-L. Bai, *ChemPhysChem*, 2003, **4**, 1114–1117.
14 J.-U. Kim, K.-H. Kim, N. Haberkorn, P. J. Roth, J.-C. Lee, P. Theato and R. Zentel, *Chem. Commun.*, 2010, **46**, 5343–5345.
15 M. R. Bockstaller, Y. Lapetnikov, S. Margel and E. L. Thomas, *J. Am. Chem. Soc.*, 2003, **125**, 5276–5277.
16 C. Park, J. Yoon and E. L. Thomas, *Polymer*, 2003, **44**, 6725–6760.
17 S.-M. Park, X. Liang, B. D. Harteneck, T. E. Pick, N. Hiroshiba, Y. Wu, B. A. Helms and D. L. Olynick, *ACS Nano*, 2011, **5**, 8523–8531.
18 J. He, C. Fang, R. A. Shelp and M. B. Zimmt, *Langmuir*, 2017, **33**, 459–467.
19 J. He, K. J. Myerson and M. B. Zimmt, *Chem. Commun.*, 2018, **46**, 3636–3639.
20 The *m*/*z* values (monoisotopic, average, observed) of the ML compounds analyzed in this study are $\mathbf{1}^{OH}$ (1126.8, 1127.7, 1127.5); **2** (1096.8, 1097.7, 1097.5); $\mathbf{1}^{SH}$ (1214.8, 1215.9, 1215.7); $\mathbf{1}^{SSA}$ (1318.8, 1320.0, 1320.5), $\mathbf{1}^{SS}\mathbf{1}$ (2428.7, 2429.7, 2432).
21 A compound's MS-TOF signal intensity depends on its desorption/ionization efficiencies and on its propensity to fragment. STM observation of excess $\mathbf{1}^{OH}$ in ML prepared from equimolar $\mathbf{1}^{OH}$/**2** solutions indicates stronger physisorption of $\mathbf{1}^{OH}$ than **2** to HOPG. Stronger $\mathbf{1}^{OH}$ adhesion contributes to the MS-TOF $\mathbf{1}^{OH}$:**2** plateau value, 0.42, from ($\mathbf{1}^{OH}\mathbf{1}^{OH}$**22**) patterned MLs being less than one.
22 B. Neises and W. Steglich, *Angew. Chem., Int. Ed.*, 1978, **17**, 522–524.
23 A laser power (LP) setting of 47% was used to quantify $\mathbf{1}^{OH}$:**2** ratios, as neither compound's ion intensity approached saturation levels (ion counts of $>75\,000$) at this power. A LP setting of 55% was needed to detect $\mathbf{1}^{SSA}$ and $\mathbf{1}^{SS}\mathbf{1}$, presumably due to their low surface concentration and heavy mass, respectively. The ion intensity from **2** reached saturation at this LP, making ion intensity ratios relative to **2** unreliable. LP settings above 55% increased fragmentation of the tetrayne chains.
24 Esterification using 5-fold higher DTBP concentration (100 mM), 2-fold lower EDC (20 mM) and the same DMAP concentration (40 mM) gave 4.5-fold higher $\mathbf{1}^{SSA}$ intensity and 10% lower $\mathbf{1}^{SS}\mathbf{1}$ intensity (Fig. S4, ESI†). The large increase of ''bimolecular product'', $\mathbf{1}^{SSA}$, but minimal change to cross-linked product, $\mathbf{1}^{SS}\mathbf{1}$, at 100 mM DTBP demonstrate cross-linking is faster than ''bimolecular'' reaction at 20 mM DTBP.
25 STM scans of TPE ML with polar groups on core chain termini (attached *in situ* or *ex situ*) exhibit excessive scratches (*e.g.* Fig. 3a).
26 W. W. Cleland, *Biochemistry*, 1964, **3**, 480–482.
27 For the preparation of (3-((3-ethoxy-3-oxopropyl)disulfaneyl)-propanoic acid) see J. Zhao, Y. Zhou, Y. Li, X. Pan, W. Zhang, N. Zhou, K. Zhang, Z. Zhang and X. Zhu, *Polym. Chem.*, 2015, **6**, 2879–2891.
28 The 4-fold smaller response factor of $\mathbf{1}^{SH}$ compared to $\mathbf{1}^{OH}$ derives from its larger mass and from additional fragmentation pathways.
29 See the ESI† for AuNP preparation, TEM and diameter histogram.
30 The plots display height fluctuation autocorrelation functions. D. Nečas and P. Klapetek, Gwyddion: An open-source software for SPM data analysis, *Cent. Eur. J. Phys.*, 2012, **10**, 181–188.
31 See ESI,† Fig. S7 for AFM scans of these control experiments.
32 The ($\mathbf{1}^{OH}\mathbf{1}^{OH}$**22**) MLs exhibit 2D-enantiomerism. The unit cell angle (between the TPE intra- and inter-column vectors) is $\sim 87^{\circ}$. Enantiomeric domains aligned along the same HOPG symmetry axis have slightly non-parallel TPE lamellae and associated AuNP strips.